3918 *Inorg. Chem.* **2010**, *49*, 3918–3926
DOI: 10.1021/ic100117y

Inorganic Chemistry
Article

Thermodynamic Studies of $[H_2Rh(diphosphine)_2]^+$ and $[HRh(diphosphine)_2(CH_3CN)]^{2+}$ Complexes in Acetonitrile

Aaron D. Wilson,[†,§] Alexander J. M. Miller,[†] Daniel L. DuBois,[*,‡] Jay A. Labinger,[*,†] and John E. Bercaw[*,†]

[†] *Arnold and Mabel Beckman Laboratories of Chemical Synthesis, California Institute of Technology, Pasadena, California 91125, and* [‡] *Chemical and Materials Sciences Division, Pacific Northwest National Laboratory, Richland, Washington 99352.* [§] *Current address: Interfacial Chemistry, Idaho National Laboratory, P.O. Box 1625, Idaho Falls, Idaho 83415*

Received January 19, 2010

Thermodynamic studies of a series of $[H_2Rh(PP)_2]^+$ and $[HRh(PP)_2(CH_3CN)]^{2+}$ complexes have been carried out in acetonitrile. Seven different diphosphine (PP) ligands were selected to allow variation of the electronic properties of the ligand substituents, the cone angles, and the natural bite angles (NBAs). Oxidative addition of H_2 to $[Rh(PP)_2]^+$ complexes is favored by diphosphine ligands with large NBAs, small cone angles, and electron donating substituents, with the NBA being the dominant factor. Large pK_a values for $[HRh(PP)_2(CH_3CN)]^{2+}$ complexes are favored by small ligand cone angles, small NBAs, and electron donating substituents with the cone angles playing a major role. The hydride donor abilities of $[H_2Rh(PP)_2]^+$ complexes increase as the NBAs decrease, the cone angles decrease, and the electron donor abilities of the substituents increase. These results indicate that if solvent coordination is involved in hydride transfer or proton transfer reactions, the observed trends can be understood in terms of a combination of two different steric effects, NBAs and cone angles, and electron-donor effects of the ligand substituents.

Introduction

Transition metal hydride complexes are important in a broad range of catalytic and stoichiometric reactions. Examples include biological catalysts such as hydrogenase enzymes, industrial catalysts such as those involved in hydroformylation of olefins, and catalysts used in the synthesis of L-Dopa for treating Parkinson's disease.[1−6] As a result, more quantitative models for understanding and predicting the thermodynamic properties of transition metal hydrides are important. For example, knowledge of the pK_a value and hydride donor ability of a transition metal hydride allows one to predict the pH range over which a transition metal hydride will be stable.[7] Similarly, hydricity of transition metal hydrides have been used to predict which hydrides generated from H_2 gas in the presence of a base will transfer a hydride ligand to coordinated CO or to BX_3 compounds.[8−11] A quantitative understanding of hydride acceptor abilities is also useful in designing electrocatalysts for H_2 production and oxidation.[12−17]

Considerations such as these have inspired efforts to measure both the kinetic and the thermodynamic hydricity of transition metal hydrides.[7,8,12,13,18−28] Many transition metal hydrides contain monodentate or bidentate phosphine ligands, and the steric and electronic properties of these

*To whom correspondence should be addressed. E-mail: daniel.dubois@pnl.gov (D.L.D.), jal@caltech.edu (J.A.L.), bercaw@caltech.edu (J.E.B.).

(1) Vineyard, B. D.; Knowles, W. S.; Sabacky, M. J.; Bachman, G. L.; Weinkauff, D. J. *J. Am. Chem. Soc.* **1977**, *99*, 5946–5952.
(2) Knowles, W. S. *Angew. Chem., Int. Ed.* **2002**, *41*, 1998–2007.
(3) Evans, D.; Osborn, J. A.; Wilkinson, G. *J. Chem. Soc., A* **1968**, 3133–3142.
(4) Esteruelas, M. A.; Oro, L. A. *Chem. Rev.* **1998**, *98*, 577–588.
(5) Fontecilla-Camps, J. C.; Volbeda, A.; Cavazza, C.; Nicolet, Y. *Chem. Rev.* **2007**, *107*, 4273–4303.
(6) Tard, C.; Pickett, C. J. *Chem. Rev.* **2009**, *109*, 2245–2274.
(7) Raebiger, J. W.; Miedaner, A.; Curtis, C. J.; Miller, S. M.; Anderson, O. P.; DuBois, D. L. *J. Am. Chem. Soc.* **2004**, *126*, 5502–5514.
(8) Mock, M. T.; Potter, R. G.; Camaioni, D. M.; Li, J.; Dougherty, W. G.; Kassel, W. S.; Twamley, B.; DuBois, D. L. *J. Am. Chem. Soc.* **2009**, *131*, 14454–14465.
(9) Ellis, W. W.; Miedaner, A.; Curtis, C. J.; Gibson, D. H.; DuBois, D. L. *J. Am. Chem. Soc.* **2002**, *124*, 1926–1932.
(10) Elowe, P. R.; West, N. M.; Labinger, J. A.; Bercaw, J. E. *Organometallics* **2009**, *28*, 6218–6227.
(11) Miller, A. J. M.; Labinger, J. A.; Bercaw, J. E. *J. Am. Chem. Soc.* **2008**, *130*, 11874–11875.
(12) Berning, D. E.; Noll, B. C.; DuBois, D. L. *J. Am. Chem. Soc.* **1999**, *121*, 11432–11447.
(13) Curtis, C. J.; Miedaner, A.; Ellis, W. W.; DuBois, D. L. *J. Am. Chem. Soc.* **2002**, *124*, 1918–1925.
(14) Berning, D. E.; Miedaner, A.; Curtis, C. J.; Noll, B. C.; Rakowski DuBois, M. C.; DuBois, D. L. *Organometallics* **2001**, *20*, 1832–1839.
(15) Curtis, C. J.; Miedaner, A.; Ciancanelli, R.; Ellis, W. W.; Noll, B. C.; Rakowski DuBois, M.; DuBois, D. L. *Inorg. Chem.* **2003**, *42*, 216–227.
(16) Wilson, A. D.; Newell, R. H.; McNevin, M. J.; Muckerman, J. T.; Rakowski DuBois, M.; DuBois, D. L. *J. Am. Chem. Soc.* **2006**, *128*, 358–366.
(17) Wilson, A. D.; Shoemaker, R. K.; Miedaner, A.; Muckerman, J. T.; DuBois, D. L.; DuBois, M. R. *Proc. Natl. Acad. Sci. U.S.A.* **2007**, *104*, 6951–6956.
(18) DuBois, D. L.; Blake, D. M.; Miedaner, A.; Curtis, C. J.; DuBois, M. R.; Franz, J. A.; Linehan, J. C. *Organometallics* **2006**, *25*, 4414–4419.
(19) Creutz, C.; Chou, M. H. *J. Am. Chem. Soc.* **2009**, *131*, 2794–2795.

 Published on Web 03/24/2010

ligands play an important role in determining the reactivity of the complexes. The steric and electronic effects can be understood in terms of parameters such as the ligand cone angle Θ and substituent parameters χ introduced by Tolman.[29] In addition to these parameters, Casey and Whiteker introduced the concept of the natural bite angle (NBA) for diphosphines as a measure of the chelate angle preferred by a given ligand backbone.[30] This concept has been elaborated extensively by van Leeuwen, Weigand, and others.[31−38] Of particular relevance to the studies reported in this work are previous thermodynamic studies of five-coordinate monohydride complexes of the type $HM(PP)_2$ (where M = Co or Rh and PP is a chelating diphosphine ligand) and $[HM'(PP)_2]^+$ (where M′ = Ni, Pd, and Pt). These studies have shown the hydride donor abilities of these complexes depend on the electron donor abilities of the substituents of the diphosphine ligand,[14] the nature of the metal,[39] and the natural bite angle (NBA) of the diphosphine ligand.[7] In contrast to these extensively studied $HM(PP)_2$ and $[HM'(PP)_2]^+$ complexes, the factors controlling the hydride donor abilities of $[H_2M(PP)_2]^+$ complexes are not known. Just as for their five-coordinate monohydride analogues, it is expected that knowledge of the factors controlling the hydride donor abilities of this class of hydrides will allow for a more rational approach to the development of catalytic and stoichiometric reactions. In this paper we interpret the thermodynamic properties of $[H_2Rh(PP)_2]^+$ and $[HRh(PP)_2(CH_3CN)]^{2+}$ complexes in terms of electronic substituent effects, ligand cone angles, and the NBAs of the diphosphine ligands.

Results

Rhodium(I) cations of the type $[Rh(PP)_2]^+$ (where PP = a diphosphine ligand) are convenient for equilibrium studies because they lie near thermoneutrality for the oxidative addition and reductive elimination of several substrates.

Scheme 1

$\Delta G°$ (kcal/mol)

$[H_2Rh(PP)_2]^+ \rightleftharpoons [Rh(PP)_2]^+ + H_2$ $1.37pK_{eq(1)}$ (1)

$[Rh(PP)_2]^+ + H^+ + CH_3CN \rightleftharpoons [HRh(PP)_2(CH_3CN)]^{2+}$ $-1.37pK_a$ (2)

$H_2 \rightleftharpoons H^+ + H^-$ 76.0 (3)

$[H_2Rh(PP)_2]^+ \rightleftharpoons [HRh(PP)_2(CH_3CN)]^{2+} + H^-$ (4)

$\Delta G°_{H^-} = 1.37pK_{eq(1)} - 1.37pK_a + 76.0$ (5)

Chart 1. List of Diphosphine (PP) Ligands and Their Abbreviations

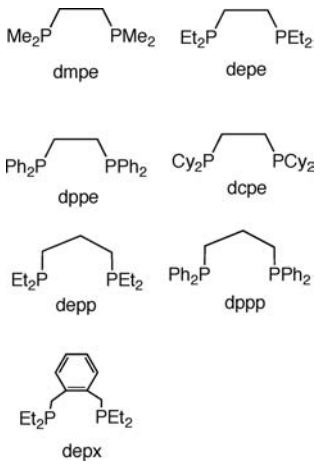

These substrates include dihalogens,[40−42] alkyl halides,[43] dioxygen,[41,42] and dihydrogen.[12−14,41] In addition, these cations can be reversibly protonated with appropriate acids in a variety of solvents.[12−14,41] Diphosphine ligands offer flexibility in backbone and substituent selection, allowing variation in the ligand bite angle as well as the steric and electronic features of the substituents.

The determination of hydride donor abilities of transition metal hydride complexes relies on the use of thermodynamic cycles such as the one shown in Scheme 1. The sum of reactions 1−3 is reaction 4, the heterolytic cleavage of the Rh−H bond of $[H_2Rh(PP)_2]^+$ to form $[HRh(PP)_2(CH_3CN)]^{2+}$, and the free energy associated with this reaction is the sum of the free energies corresponding to reactions 1−3 as shown in eq 5. The determinations of the equilibrium constants associated with reaction 1 and the pK_a values for reaction 2 for complexes containing the diphosphine ligands in Chart 1 are discussed below. The free energy for the heterolytic cleavage of H_2 in acetonitrile (reaction 3, 76.0 kcal/mol) was taken from reference 49. The stereochemistry for reaction 1 is shown in reaction 1′ below.

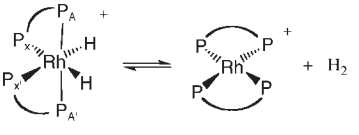

1 2 (1′)

Determination of the Free Energy of Hydrogen Elimination ($\Delta G°_{-H2}$) from $[H_2Rh(PP)_2]^+$ Complexes. It was

(20) Miedaner, A.; Raebiger, J. W.; Curtis, C. J.; Miller, S. M.; DuBois, D. L. *Organometallics* **2004**, *23*, 2670–2679.
(21) Raebiger, J. W.; DuBois, D. L. *Organometallics* **2005**, *24*, 110–118.
(22) Price, A. J.; Ciancanelli, R.; Noll, B. C.; Curtis, C. J.; DuBois, D. L.; DuBois, M. R. *Organometallics* **2002**, *21*, 4833–4839.
(23) Ciancanelli, R.; Noll, B. C.; DuBois, D. L.; DuBois, M. R. *J. Am. Chem. Soc.* **2002**, *124*, 2984–2992.
(24) Curtis, C. J.; Miedaner, A.; Raebiger, J. W.; DuBois, D. L. *Organometallics* **2004**, *23*, 511–516.
(25) Dedieu, A. *Transition Metal Hydrides*; John Wiley & Sons: New York, 1991.
(26) Cheng, T.; Bullock, R. M. *Organometallics* **1995**, *14*, 4031–4033.
(27) Cheng, T.; Bullock, R. M. *Organometallics* **2002**, *21*, 2325–2331.
(28) Cheng, T.; Bullock, R. M. *J. Am. Chem. Soc.* **1999**, *121*, 3150–3155.
(29) Tolman, C. A. *Chem. Rev.* **1977**, *77*, 313–348.
(30) Casey, C. P.; Whiteker, G. T. *Isr. J. Chem.* **1990**, *30*, 299–304.
(31) van der Veen, L. A.; Boele, M. D. K.; Bregman, F. R.; Kamer, P. C. J.; van Leeuwen, P. W. N. M.; Goubitz, K.; Fraanje, J.; Schenk, H.; Bo, C. *J. Am. Chem. Soc.* **1998**, *120*, 11616–11626.
(32) Dierkes, P.; Leeuwen, P. W. N. M. V. *J. Chem. Soc., Dalton Trans.* **1999**, 1519–1530.
(33) van der Veen, L. A.; Keeven, P. H.; Schoemaker, G. C.; Reek, J. N. H.; Kamer, P. C. J.; van Leeuwen, P. W. N. M.; Lutz, M.; Spek, A. L. *Organometallics* **2000**, *19*, 872–883.
(34) van Leeuwen, P. W. N. M.; Kamer, P. C. J.; Reek, J. N. H.; Dierkes, P. *Chem. Rev.* **2000**, *100*, 2741–2770.
(35) Freixa, Z.; Leeuwen, P. W. N. M. V. *Dalton Trans.* **2003**, 1890–1901.
(36) van Zeist, W.; Visser, R.; Bickelhaupt, F. *Chem.—Eur. J.* **2009**, *15*, 6112–6115.
(37) Aguila, D.; Escribano, E.; Speed, S.; Talancon, D.; Yerman, L.; Alvarez, S. *Dalton Trans.* **2009**, ASAP.
(38) Niksch, T.; Görls, H.; Weigand, W. *Eur. J. Inorg. Chem.* **2009**, ASAP.
(39) Curtis, C. J.; Miedaner, A.; Raebiger, J. W.; DuBois, D. L. *Organometallics* **2004**, *23*, 511–516.
(40) Chatt, J.; Butter, S. A. *Chem. Commun.* (*London*) **1967**, 501–502.
(41) Butter, S. A.; Chatt, J. *J. Chem. Soc., A* **1970**, 1411–1415.
(42) Suzuki, T.; Isobe, K.; Kashiwabara, K. *J. Chem. Soc., Dalton Trans.* **1995**, 3609–3616.
(43) Marder, T. B.; Fultz, W. C.; Calabrese, J. C.; Harlow, R. L.; Milstein, D. *J. Chem. Soc., Chem. Commun.* **1987**, 1543–1545.

Table 1. $^{31}P\{^1H\}$ NMR Data and ^1H NMR Hydride Data and Assignments for $[Rh(PP)_2]^+$, $[H_2Rh(PP)_2]^+$, and $[HRh(PP)_2(CH_3CN)]^{2+}$ Complexes

complex	^{31}P NMR (δ)	^1H NMR hydride peak (δ)
$[Rh(dmpe)_2]^+$	36.4, $^1J_{RhP}$ 123 Hz	N/A
$[Rh(depe)_2]^+$	63.2, $^1J_{RhP}$ 126 Hz	N/A
$[Rh(dppe)_2]^+$	58.5, $^1J_{RhP}$ 133 Hz	N/A
$[Rh(dcpe)_2]^+$	67.1, $^1J_{RhP}$ 131 Hz	N/A
$[Rh(dppb)_2]^+$	62.5, $^1J_{RhP}$ 134 Hz	N/A
$[Rh(depp)_2]^+$	5.0, $^1J_{RhP}$ 126 Hz	N/A
$[Rh(dppp)_2]^+$	8.4, $^1J_{RhP}$ 132 Hz	N/A
$[Rh(depx)_2]^{+a}$	12.7, $^1J_{RhP}$ 134 Hz	N/A
$[H_2Rh(dmpe)_2]^+$	38.0 br, 26.4 br	−10.3 br d, *trans* $^2J_{PH}$ 145 Hz
$[H_2Rh(depe)_2]^+$	64.5 br, 47.5 br	−10.7 br d, *trans* $^2J_{PH}$ 132 Hz
$[H_2Rh(dppe)_2]^+$	63.3 br, 46.9 br	−9.0 br d, *trans* $^2J_{PH}$ 152 Hz
$[H_2Rh(dcpe)_2]^+$	74.6 dt, $^1J_{RhP}$ 96 Hz, $^2J_{PP}$ 14 Hz, 50.5 br	−12.5 br d, *trans* $^2J_{PH}$ 140 Hz
$[H_2Rh(dppb)_2]^+$	N/A	N/A
$[H_2Rh(depp)_2]^+$	15.0 dt, $^1J_{RhP}$ 94 Hz, $^2J_{PP}$ 30 Hz −6.1 dt, $^1J_{RhP}$ 81 Hz, $^2J_{PP}$ 30 Hz	−10.8 br d, *trans* $^2J_{PH}$ 140 Hz
$[H_2Rh(dppp)_2]^+$	18.9 dt, $^1J_{RhP}$ 100 Hz, $^2J_{PP}$ 30 Hz 7.0 dt, $^1J_{RhP}$ 83 Hz, $^2J_{PP}$ 30 Hz	−8. br d, *trans* $^2J_{PH}$ 141 Hz
$[H_2Rh(depx)_2]^{+a}$	15.7 br, 3.4 ppm br	−10.8 br d, *trans* $^2J_{PH}$ 142 Hz
$[HRh(dmpe)_2(CH_3CN)]^{2+}$	38.0, $^1J_{RhP}$ 88 Hz	−18.5 dp, $^1J_{RhH}$ 14 Hz, $^2J_{PH}$ 14 Hz
$[HRh(depe)_2(CH_3CN)]^{2+}$	58.4, $^1J_{RhP}$ 87 Hz	−18.3 dp, $^1J_{RhH}$ 16 Hz, $^2J_{PH}$ 12 Hz
$[HRh(dppe)_2(CH_3CN)]^{2+}$	56.0, $^1J_{RhP}$ 92 Hz	−15.9 dp, $^1J_{RhH}$ 11 Hz, $^2J_{PH}$ 11 Hz
$[HRh(dcpe)_2(CH_3CN)]^{2+}$	63.9, $^1J_{RhP}$ 88 Hz	−19.1 dp, $^1J_{RhH}$ 10 Hz, $^2J_{PH}$ 10 Hz
$[HRh(dppb)_2(CH_3CN)]^{2+}$	56.9, $^1J_{RhP}$ 93 Hz	−14.6 dp, $^1J_{RhH}$ 10 Hz, $^2J_{PH}$ 7.5 Hz
$[HRh(depp)_2(CH_3CN)]^{2+}$	4.8, $^1J_{RhP}$ 85 Hz	−17.6 dp, $^1J_{RhH}$ 15 Hz, $^2J_{PH}$ 14 Hz
$[HRh(dppp)_2(CH_3CN)]^{2+}$	6.2, $^1J_{RhP}$ 91 Hz	−14.9 dp, $^1J_{RhH}$ 12 Hz, $^2J_{PH}$ 12 Hz
$[HRh(depx)_2(CH_3CN)]^{2+a}$	*cis*: 26.4, 9.4, −2.0, −18.3 *trans*: 25.4 and 19.6	*cis*: −10.3, $^2J_{PH}$ 163 Hz *trans*: −18.6 br s

[a] Data from reference 21.

previously reported that $[H_2Rh(dmpe)_2]^+$ and $[H_2Rh(depe)_2]^+$ reversibly lose hydrogen as shown in reaction 1′, with equilibrium constants of 0.6 and 4.0 atm, respectively.[18] The complex $[H_2Rh(dppp)_2]^+$ is also in equilibrium with $[Rh(dppp)_2]^+$ under 1.0 atm of hydrogen, and the $^{31}P\{^1H\}$ NMR spectrum of $[H_2Rh(dppp)_2]^+$ exhibits two doublets of triplets indicating an AA′XX′M spin system and a *cis* geometry. Integration of the ^{31}P NMR resonances of **1** and **2** can be used to determine an equilibrium constant of 0.10 atm for reaction 1 when the diphosphine ligand is dppp. A listing of the observed $^{31}P\{^1H\}$ NMR resonances and their assignments are provided in Table 1 for the $[Rh(PP)_2]^+$ and $[H_2Rh(PP)_2]^+$ complexes discussed in this paper.

The complex $[Rh(dppe)_2]^+$ does not react with H_2 at 1.0 atm; however, at 110 atm H_2, sufficient $[H_2Rh(dppe)_2]^+$ is observed in equilibrium with $[Rh(dppe)_2]^+$ to permit accurate integration of the two rhodium species. An equilibrium constant of 5.7×10^2 atm was determined, corresponding to a $\Delta G°_{-H2}$ value of −3.8 kcal/mol. Similarly measurable amounts of $[H_2Rh(dcpe)_2]^+$ were produced from $[Rh(dcpe)_2]^+$ at H_2 pressures greater than 130 atm. A broad resonance at 50.5 ppm is assigned to the phosphorus atoms *trans* to the hydride ligands (P_X and $P_{X'}$ of structure **1**). This assignment is supported by the HSQC NMR data, with the observation of a prominent cross peak between the hydride at −12.5 ppm on the ^1H axis and the resonance at 50.5 ppm on the ^{31}P NMR axis. This signal can be assigned with confidence because of the large (∼140 Hz) *trans* $^2J_{PH}$. The area of the ^{31}P resonance at 50.5 ppm correlates with a relatively sharp doublet of triplets at 74.6 ppm attributed to P_A and $P_{A'}$ of structure **1**. The *cis* phosphorus atoms (P_A and $P_{A'}$ of structure **1**) did not display a cross peak with the hydride. This is attributed to the smaller *cis* $^2J_{PH}$ (∼15 Hz) and H_2 exchange. In addition to the resonances assigned to $[H_2Rh(dcpe)_2]^+$ (**1**) and $[Rh(dcpe)_2]^+$ (**2**), resonances were observed at 92.6 ppm ($^1J_{RhP}$ 186 Hz) and at 52.2 ppm with no rhodium coupling. The former is tentatively attributed to $[Rh(dcpe)(CH_3CN)_2]^+$ and the latter to a ligand decomposition product. Despite these additional species, a reproducible equilibrium constant of 1.0×10^3 atm was obtained for reaction 1 over the range of hydrogen pressures studied (110−140 atm).

A solution of $[Rh(dppb)_2]^+$ was subjected to H_2 pressures greater than 130 atm, but no oxidative addition product was observed; hence the dissociation free energy of $[H_2Rh(dppb)_2]^+$ is more negative than −4.4 kcal/mol. At the opposite extreme, $[Rh(depp)_2]^+$ and $[Rh(depx)_2]^+$ add H_2 irreversibly at 1.0 atm H_2. Because no equilibrium is observed, the free energy of hydrogen elimination for $[H_2Rh(depp)_2]^+$ and $[Rh(depx)_2]^+$ must be derived indirectly, as discussed below under the topic of hydride donor abilities. The free energies ($\Delta G°_{-H2}$) associated with reaction 1 for the $[H_2Rh(PP)_2]^+$ complexes discussed in the preceding paragraphs and those available for $[H_2Rh(depx)_2]^+$ from the literature[21] are summarized in column 5 of Table 2.

Determination of pK_a Values for $[HRh(PP)_2(CH_3CN)]^{2+}$ Complexes. In addition to the equilibrium constants for reaction 1, determination of the hydride donor abilities of $[H_2Rh(PP)_2]^+$ complexes using Scheme 1 requires pK_a values for the cationic rhodium $[HRh(PP)_2(CH_3CN)]^{2+}$ complexes. The pK_a values for the complexes containing the ligands in Chart 1 were determined by using Scheme 2. In a typical experiment, an acetonitrile solution of $[Rh(PP)_2]^+$ was treated with a mixture of an acid and its conjugate base, and monitored by $^{31}P\{^1H\}$ NMR spectroscopy until equilibrium was achieved. Equilibrium constants for eq 6 were determined by integration of the ^{31}P NMR resonances of the equilibrating rhodium species and mass balance of the acid/conjugate

Table 2. Thermodynamic Data and Ligand Parameters for $[Rh(PP)_2]^+$, $[H_2Rh(PP)_2]^+$, and $[HRh(PP)_2(CH_3CN)]^{2+}$ Complexes[a]

PP	Θ_B[b] (deg)	NBA[c] (deg)	TEM[d] $\Sigma^3\chi$	$[H_2Rh(PP)_2]^+$ $\Delta G°_{-H2}$ kcal/mol (eq 1)	$[H_2Rh(PP)_2]^+$ $\Delta G°_{H^-}$ kcal/mol (eq 5)	$[HRh(PP)_2(MeCN)]^{2+}$ $\Delta G°_{H+}$ kcal/mol (pK_a) (eq 9)
dmpe	107 (107)	86	7.8	+0.44[e]	50.4	26.0 (18.9)
depe	117 (115)	86	6.2	−0.87[e]	52.3	22.8 (16.6)
dppe	125 (125)	86	11.2	−3.8	59.6	12.3 (9.0)[e]
dcpe	142 (142)	86	2.8	−4.2	63.1	8.7 (6.0)
depp	119	93	6.2	+5.1	61.3	19.8 (14.4)
depx	121	100	6.2	+11.4[f]	71.6[f]	15.8 (11.5)[f] (6:1 *cis* to *trans*)
dppb	125	86	12.9	< −4.4	< 58.7	12.9 (9.4)[e]
dppp	127 (127)	93	11.2	+1.4	69.5	7.9 (5.8)

[a] All values are for acetonitrile at 23 ± 2 °C. [b] From eq 15 as discussed in the Supporting Information, values in parentheses are from reference 29. [c] Ref 37. [d] Tolman electronic parameters from ref 29, as discussed in the Supporting Information. [e] Ref 18. [f] Ref 21, weighted average of *cis* and *trans* values.

Scheme 2

$$[HRh(PP)_2(MeCN)]^{2+} + Base \rightleftharpoons [Rh(PP)_2]^{+} + HBase^{+} + MeCN \quad (6)$$

$$HBase^{+} \rightleftharpoons Base + H^{+} \quad (7)$$

$$[HRh(PP)_2(MeCN)]^{2+} \rightleftharpoons [Rh(PP)_2]^{+} + H^{+} + MeCN \quad (8)$$

$$pK_a(HRh) = pK_a(HBase^{+}) + pK_{eq(6)} \quad (9)$$

base pair. (Details are discussed in the Experimental Section.) These equilibrium constants, together with published pK_a data for acids in acetonitrile (eq 7),[9,44−48] were used to calculate the pK_a values of the corresponding $[HRh(PP)_2(CH_3CN)]^{2+}$ complexes using eq 9. The resulting values and the corresponding free energies for deprotonation of $[HRh(PP)_2(CH_3CN)]^{2+}$ are summarized in column 7 of Table 2. It is worth noting that in reactions 6 and 8, deprotonation of the $[HRh(PP)_2(CH_3CN)]^{2+}$ complex is accompanied by loss of acetonitrile. For these reactions, the activity of pure acetonitrile solvent is taken as unity. This choice of standard states results in pK_a values that are internally consistent with pK_a values reported for complexes in acetonitrile that do not involve solvent loss. However, the pK_a values calculated according to Scheme 2 cannot be readily transferred to solvents other than acetonitrile.

Determination of the Hydride Donor Ability ($\Delta G°_{H^-}$) of $[H_2Rh(PP)_2]^+$ Complexes. The equilibrium constants for H_2 loss and the pK_a values for reaction 2 were used to calculate the hydride donor abilities of the $[H_2Rh(PP)_2]^+$ complexes using Scheme 1, with the exception of $[H_2Rh(depp)_2]^+$. The $\Delta G°_{H^-}$ values are shown in Table 2. Because $[Rh(depp)_2]^+$ reacts irreversibly with H_2, Scheme 1 could not be used to determine the hydride donor ability of $[H_2Rh(depp)_2]^+$. In this case, the hydride donor ability was determined using Scheme 3, where the free energy for the heterolytic cleavage of H_2 in acetonitrile (eq 12) was taken from the literature.[49] In contrast, $[Rh(dppb)_2]^+$ does not react with H_2 even at 140 atm. As a result, the value of $\Delta G°_{H^-}$ for this complex can only be determined to be less than 58.7 kcal/mol.

Scheme 3

$$[H_2Rh(PP)_2]^{+} + HBase^{+} + MeCN \rightleftharpoons [HRh(PP)_2(MeCN)]^{2+} + Base + H_2 \quad \Delta G° \text{ (kcal/mol)}: 1.37pK_{eq(10)} \quad (10)$$

$$Base + H^{+} \rightleftharpoons HBase^{+} \quad \Delta G°: -1.37pK_a(HBase^{+}) \quad (11)$$

$$H_2 \rightleftharpoons H^{+} + H^{-} \quad \Delta G°: 76.0 \quad (12)$$

$$[H_2Rh(PP)_2]^{+} + MeCN \rightleftharpoons [HRh(PP)_2(MeCN)]^{2+} + H^{-} \quad (13)$$

$$(\Delta G°_{H^-}) = 1.37pK_{eq(10)} - 1.37pK_a(HBase^{+}) + 76.0 \quad (14)$$

Discussion

The objective of this work is to delineate the ligand parameters controlling various thermodynamic properties of $[H_2Rh(PP)_2]^+$ and $[HRh(PP)_2(CH_3CN)]^{2+}$ complexes. Previous studies of $[HM(PP)_2]^+$ complexes (where M = Ni, Pd, and Pt) have shown that the hydride donor abilities, pK_a values, and homolytic solution bond dissociation free energies depend on three factors. These are the nature of the metal, the electron donor or acceptor ability of the substituents on the diphosphine ligand, and the natural bite angle of the ligand.[39] In contrast, although thermodynamic hydride donor abilities have been reported for a small number of six-coordinate metal complexes,[19,50−53] there has been no systematic study of this class. The ligands shown in Chart 1 were selected because they provide a range of cone angles, natural bite angles, and electronic parameters as shown in columns 2−4 of Table 2.

Reductive Elimination of H_2 from $[H_2Rh(PP)_2]^+$ Complexes. The reductive elimination of H_2 from distorted cis-octahedral $[H_2Rh(PP)_2]^+$ complexes results in the formation of $[Rh(PP)_2]^+$ complexes. The NBAs appear to be the dominant factor influencing this reaction and its reverse, the oxidative addition of H_2 to $[Rh(PP)_2]^+$. For example, elimination of H_2 is favored by 12.3 kcal/mol for $[H_2Rh(depe)_2]^+$ ($\Delta G°_{-H2}$ = −0.87 kcal/mol) compared to $[H_2Rh(depx)_2]^+$ (11.4 kcal/mol), which have NBAs of 86° and 100°, respectively.[37] This effect has been discussed previously and can be understood in terms of simple molecular orbital overlap arguments, in which the tetrahedral distortion from a square-planar geometry associated

(44) Kaljurand, I.; Kutt, A.; Soovali, L.; Rodima, T.; Maemets, V.; Leito, I.; Koppel, I. A. *J. Org. Chem.* **2005**, *70*, 1019–1028.
(45) Kolthoff, I. M.; Chantooni, M. K.; Bhowmik, S. *Anal. Chem.* **1967**, *39*, 1627–1633.
(46) Menger, F. M.; Williams, R. F. *J. Org. Chem.* **1974**, *39*, 2131–2133.
(47) Kolthoff, I. M.; Bruckenstein, S.; Chantooni, M. K. *J. Am. Chem. Soc.* **1961**, *83*, 3927–3935.
(48) Kutt, A.; Leito, I.; Kaljurand, I.; Soovali, L.; Vlasov, V. M.; Yagupolskii, L. M.; Koppel, I. A. *J. Org. Chem.* **2006**, *71*, 2829–2838.
(49) Wayner, D. D. M.; Parker, V. D. *Acc. Chem. Res.* **1993**, *26*, 287–294.
(50) Ellis, W. W.; Ciancanelli, R.; Miller, S. M.; Raebiger, J. W.; Rakowski DuBois, M.; DuBois, D. L. *J. Am. Chem. Soc.* **2003**, *125*, 12230–12236.
(51) Wei, M.; Wayland, B. B. *Organometallics* **1996**, *15*, 4681–4683.
(52) Fu, X.; Wayland, B. B. *J. Am. Chem. Soc.* **2004**, *126*, 2623–2631.
(53) Fu, X.; Li, S.; Wayland, B. B. *Inorg. Chem.* **2006**, *45*, 9884–9889.

with a larger NBA results in a decrease of the energy of the σ acceptor orbital and an increase in the energies of the π-donor orbitals of the $[Rh(PP)_2]^+$ complex.[7,12,54] These changes in orbital energies favor the addition of hydrogen to $[Rh(PP)_2]^+$ derivatives as the NBAs increase.

When considering the effect of the steric bulk of the ligand substituents, it is not obvious whether sterically bulky groups will favor either $[H_2Rh(PP)_2]^+$ or $[Rh(PP)_2]^+$. Tolman introduced the concept of cone angle to quantify the bulkiness of various substituents, and values have been published for the cone angles of the diphosphine ligands with ethylene backbones used in this study (shown in parentheses in Table 2). Tolman calculated the cone angle for diphosphine ligands (Θ_B) using eq 15, where Θ_M is the cone angle of the corresponding monodentate PR_3 ligand with the same R substituents as the diphosphine ligands and α is the experimentally observed PMP bond angle of the chelating diphosphine ligand. We have extended this method to the other ligands shown in Chart 1 using the experimentally determined bite angles from the work of Aguila et al.[37] and the cone angles for the corresponding monodentate ligands used by Tolman (see Supporting Information).[29] Our calculated values are the same as those reported by Tolman for the ligands previously reported with the exception of depe for which we calculate a cone angle of 117° versus Tolman's 115°. This approach allows cone angles that are consistent with those used by Tolman to be determined for the additional ligands used in this work.

$$\Theta_B = 2/3(\Theta_M + 1/2\alpha) \quad (15)$$

A plot of $\Delta G°_{-H2}$ versus the cone angle for the data in Table 2 is shown in Figure 1. It can be seen that the data for the ligands with an ethylene backbone are nearly colinear (see solid line), and increasing the steric bulk of the substituents clearly favors reductive elimination of H_2. It is of interest to note that this steric effect is counter to that observed for increasing the natural bite angle. It is also apparent from Figure 3 that the data point for the dppe complex deviates slightly from the value expected based on pure steric considerations, and this small deviation of −2.1 kcal/mol is attributed to electronic effects. The poorer electron donating ability of the phenyl substituents compared to the alkyl substituents favors reductive elimination of H_2. This electronic effect has been noted previously.[55−57] In summary, oxidative addition of H_2 to $[Rh(PP)_2]^+$ complexes is favored by diphosphine ligands with large NBAs, small cone angles, and electron donating substituents, with the NBA being the dominant factor.

pK_a Values of $[HRh(PP)_2(CH_3CN)]^{2+}$ Complexes. Protonation of $[Rh(PP)_2]^+$ cations in acetonitrile is accompanied by the coordination of a solvent molecule and results in the formation of *trans*-$[HRh(PP)_2(CH_3CN)]^{2+}$ complexes. As a result, it is expected that factors influencing the dissociation of the solvent ligand will influence

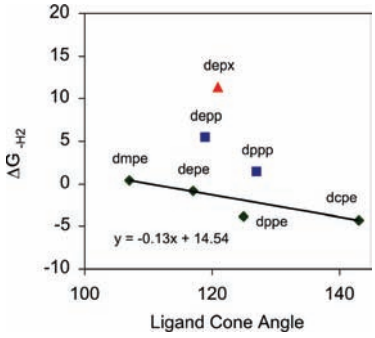

Figure 1. Plot of $\Delta G°_{-H2}$ versus the cone angle for the data in Table 2. The diphosphine ligands of the corresponding *cis*-$[H_2Rh(PP)_2]^+$ complexes are shown adjacent to each data point with the green diamonds corresponding to ligands with ethylene backbones, the blue squares to propylene backbones, and the red triangle to that for depx which contains four carbon atoms.

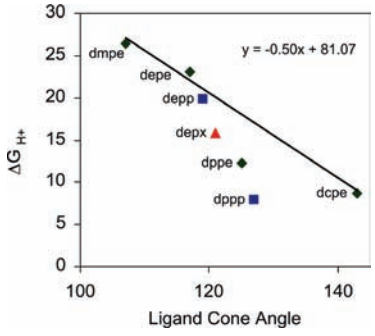

Figure 2. Plot of $\Delta G°_{H+}$ for $[HRh(PP)_2(CH_3CN)]^{2+}$ complexes versus the cone angle of the corresponding diphosphine ligands. The straight line is the best fit line through the data for the diphosphine ligands containing ethylene backbones and alkyl substituents.

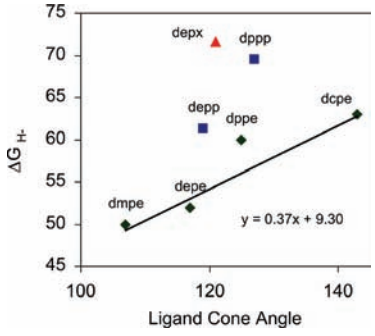

Figure 3. Plot of $\Delta G°_{H-}$ versus the ligand cone angle. The solid line is the best-fit line through the data for the ligands with ethylene backbones and alkyl substituents.

the free energies ($\Delta G°_{H+}$) and pK_a values associated with deprotonation of the corresponding *trans*-$[HRh(PP)_2(CH_3CN)]^{2+}$ complexes. These values are shown in column 7 of Table 2, and Figure 2 shows a plot of $\Delta G°_{H+}$ versus the cone angles of the diphosphine ligands. The solid line represents the best-fit line for the diphosphine ligands with an ethylene backbone and alkyl substituents. The $\Delta G°_{H+}$ value of $[HRh(dmpe)_2(CH_3CN)]^{2+}$ is 17.3 kcal/mol larger than that of $[HRh(dcpe)_2(CH_3CN)]^{2+}$, indicating that the cone angles of the diphosphine ligands play a major role in determining the pK_a values of these complexes. Steric interactions between the phosphine substituents and the acetonitrile ligand that coordinates upon protonation of the metal

(54) Miedaner, A.; Haltiwanger, R. C.; DuBois, D. L. *Inorg. Chem.* **1991**, *30*, 417–427.
(55) Hartwig, J. F. *Inorg. Chem.* **2007**, *46*, 1936–1947.
(56) Abis, L.; Santi, R.; Halpern, J. *J. Organomet. Chem.* **1981**, *215*, 263–267.
(57) Jones, W. D.; Kuykendall, V. L. *Inorg. Chem.* **1991**, *30*, 2615–2622.

apparently results in less stable and more acidic *trans*-$[HRh(PP)_2(CH_3CN)]^{2+}$ complexes. An analogous explanation, based on counterbalancing steric and electronic effects, has been offered to account for the unexpected similarity in the thermodynamic hydride donor abilities of $[HW(CO)_4P(OMe_3)]^-$ (37 kcal/mol) and $[HW(CO)_4(PPh_3)]^-$ (36 kcal/mol).[50]

Comparison of the values for depe, depp, and depx complexes and of dppe and dppp complexes indicates that an increase in the NBA also increases the acidity of these complexes, but this effect is smaller than the effect of the cone angle. Both trends are understandable in terms of increased steric interactions between the diphosphine ligands, and between the diphosphine ligands and acetonitrile, as the NBA or cone angle increases. In contrast, as discussed above, oxidative addition of H_2 to $[Rh(PP)_2]^+$ complexes is significantly favored by an increase in the NBA of the diphosphine ligands, but disfavored by an increase of the steric bulk of the ligands cone angle. This difference in the dependence of the driving force for the oxidative addition of H_2 to $[Rh(PP)_2]^+$ and protonation of $[Rh(PP)_2]^+$, both of which result in an increase in the formal oxidation state and the coordination number of the metal by two, is thought to arise from the different geometries (*cis* and *trans*) of the two products formed.

The value of $\Delta G°_{H+}$ for *trans*-$[HRh(dppe)_2(CH_3CN)]^{2+}$, which has phenyl substituents, is significantly smaller than expected for an alkyl-substituted complex with the same cone angle. The −5.9 kcal/mol difference between the expected and observed values for dppe is attributed to the difference in the electron-donor ability of phenyl groups compared to alkyl groups. For comparison, the $\Delta G°_{H+}$ value for $[HM(depe)_2]^+$ is 14 or 10 kcal/mol larger than that of $[HM(dppe)_2]^+$ for M = Ni and Pt, respectively. These values for nickel and platinum are primarily determined by the electron donor abilities of the substituents, not the NBAs or cone angles. Apparently electronic substituent effects are relatively less important (compared to steric effects) in determining the acidities of $[HRh(PP)_2(CH_3CN)]^{2+}$ complexes than those of the $[HM(PP)_2]^+$ complexes of nickel and platinum; presumably this is in large part a consequence of the sixth ligand in the former. In summary, large pK_a values for $[HRh(PP)_2(CH_3CN)]^{2+}$ complexes are favored by small ligand cone angles, small NBAs, and electron donating substituents with both cone angles and electron donor abilities playing a major role.

Hydride Donor Abilities of $[H_2Rh(PP)_2]^+$ Complexes. Column 6 in Table 2 lists the hydride donor abilities ($\Delta G°_{H-}$) of $[H_2Rh(PP)_2]^+$ complexes, which measure the thermodynamic driving force for dissociation of a hydride ligand from the dihydride to form $[HRh(PP)_2(CH_3CN)]^{2+}$. Smaller values of $\Delta G°_{H-}$ indicate a greater driving force for the delivery of a hydride by $[H_2Rh(PP)_2]^+$ complexes. As can be seen from Table 2, the hydride donor abilities of the complexes range from 50.4 kcal/mol for $[H_2Rh(dmpe)_2]^+$ to 71.6 kcal/mol for $[H_2Rh(depx)_2]^+$. Because the pK_a values of $[HRh(PP)_2(CH_3CN)]^{2+}$ and the $\Delta G°_{-H2}$ values of $[H_2Rh(PP)_2]^+$ are used to calculate the $\Delta G°_{H-}$ values of $[H_2Rh(PP)_2]^+$, it is anticipated that both electronic and steric effects will make significant contributions to the hydride donor abilities of $[H_2Rh(PP)_2]^+$ complexes.

The observation that $[H_2Rh(dmpe)_2]^+$ is a better hydride donor than $[H_2Rh(dcpe)_2]^+$ by 12.7 kcal/mol suggests that the cone angle of the diphosphine ligand exerts a significant influence on the hydride donor abilities of these complexes. This is illustrated graphically in Figure 3 by the linear dependence of the plot of $\Delta G°_{H-}$ versus the ligand cone angle for the ligands with ethylene backbones and alkyl substituents (solid line). Ligands with larger cone angles give complexes with poorer hydride donor abilities or larger $\Delta G°_{H-}$ values. This can be understood in terms of increased steric interactions between acetonitrile and diphosphine ligands with larger cone angles. This interaction disfavors the binding of acetonitrile that accompanies hydride ligand loss. For the ethylene bridged ligands, dppe deviates from the best-fit line for the alkyl substituted ligands by 4.0 kcal/mol. This is attributed to electronic effects with phenyl substituents resulting in poorer hydride donors than alkyl substituents, and this electronic effect is comparable to the difference in the $\Delta G°_{H+}$ values for the $[HRh(PP)_2(CH_3CN)]^{2+}$ complexes discussed in the preceding section. The NBA also plays an important role in determining the hydride donor ability of $[H_2Rh(PP)_2]^+$ complexes. The complex $[H_2Rh(depe)_2]^+$ is a better hydride donor than $[H_2Rh(depx)_2]^+$ by 19.3 kcal/mol. If this difference is corrected for electronic effects of ethyl versus benzyl, this difference would be expected to be slightly smaller (1−2 kcal/mol). In summary, the hydride donor abilities of $[H_2Rh(PP)_2]^+$ complexes increase as the NBAs decrease, the cone angles decrease, and the electron donor abilities of the substituents increase. In this case the influence of the NBAs and cone angles appear to be of comparable magnitude and dominate electronic effects of the substituents.

Comparison with Other Metal Hydride Systems. Previously reported thermodynamic studies of metal complexes most relevant to those reported here include the $[H_2Co(dppe)_2]^+$ and $[H_2Pt(EtXantphos)_2]^{2+}$ systems. $[H_2Co(dppe)_2]^+$ is reported to have a $\Delta G°_{-H2}$ of 4.6 kcal/mol while $[H_2Rh(dppe)]^+$ has a $\Delta G°_{-H2}$ of −4.0 kcal/mol. This indicates that oxidative addition of H_2 to $[Co(dppe)_2]^+$ is favored over the oxidative addition of H_2 to $[Rh(dppe)_2]^+$ by 8.6 kcal/mol. Although this is only one direct comparison, the conclusion that $[Co(PP)_2]^+$ complexes will bind H_2 more strongly than $[Rh(PP)_2]^+$ for the same diphosphine ligand is likely to be generally valid. The pK_a value of 11.3 for $[HCo(dppe)_2(CH_3CN)]^{2+}$ compared to 9.0 for $[HRh(dppe)_2(CH_3CN)]^{2+}$ indicates that rhodium is slightly more acidic than cobalt in these six coordinate structures. $[H_2Co(dppe)]^+$ ($\Delta G°_{H-}$ = 65.1 kcal/mol) is a significantly less powerful hydride donor than $[H_2Rh(dppe)]^+$ ($\Delta G°_{H-}$ = 59.6 kcal/mol), but this difference is smaller than that observed between first and second row metals in five coordinate monohydride $[HM(PP)_2]^+$ complexes, for which palladium complexes are generally 15 kcal/mol better hydride donors than the corresponding nickel complexes.

Group 10 d^6 bis(diphosphine) dihydrides are uncommon; nonetheless one example, $[H_2Pt(EtXantphos)_2]^{2+}$ [EtXantphos = 9,9-dimethyl-4,5-bis(diethylphosphino)-xanthene], has been observed by NMR.[20] This complex has a $\Delta G°_{-H2}$ of 9.3 kcal/mol. Consistent with the rhodium trends, this $[H_2Pt(PP)_2]^{2+}$ species is one with an

extremely large bite angle. Despite the significant driving force for the formation of $[H_2Pt(EtXantphos)_2]^{2+}$, it still takes days for 1 atm of hydrogen to completely consume $[Pt(EtXantphos)_2]^{2+}$. In contrast, the reactions of H_2 with $[Rh(PP)_2]^+$ derivatives are fast (complete prior to taking NMR spectra) in all cases reported here, even those with very little driving force. While reaction kinetics have not been explicitly evaluated in this work, it is clear that there is a significant difference in the intrinsic activation barriers for the addition of hydrogen to $[Rh(PP)_2]^+$ and $[Pt(PP)_2]^{2+}$.

Comparison with Five-Coordinate $HRh(PP)_2$ Complexes. $HRh(PP)_2$ complexes can be generated by the deprotonation of $[H_2Rh(PP)_2]^+$, and the hydride donor abilities of the five coordinate hydrides have been investigated for four different ligands; dmpe ($\Delta G°_{H^-}$ = 26.4 kcal/mol), depe ($\Delta G°_{H^-}$ = 28.1 kcal/mol), dppb ($\Delta G°_{H^-}$ = 33.9 kcal/mol), and depx ($\Delta G°_{H^-}$ = 45 kcal/mol).[18,21,22] Comparisons of these values with those of the corresponding $[H_2Rh(PP)_2]^+$ derivatives indicate that deprotonation of the dihydride complexes results in the formation of a monohydride complex that is approximately a 25 kcal/mol better hydride donor. If both the $[H_2Rh(PP)_2]^+$ and $HRh(PP)_2$ complexes are considered, the hydride donor abilities demonstrated for $HRh(dmpe)_2$ and $[H_2Rh(depx)_2]^+$span a range of 45 kcal/mol. This range of hydride donor abilities can be accessed readily from H_2 gas and bases of various strengths.

Conclusions

The thermodynamic studies described above demonstrate that while both steric and electronic influences of diphosphine ligands are factors, the steric constraints of the cone and bite angle tend to dominate the thermodynamic properties of six-coordinate rhodium hydride complexes. As expected, electron donating substituents on the diphosphine ligands increase pK_a values of $[HRh(PP)_2(CH_3CN)]^{2+}$, correlate with better hydride donor abilities of $[H_2Rh(PP)_2]^+$, and disfavor reductive elimination of H_2 from $[H_2Rh(PP)_2]^+$. Larger NBAs decrease the pK_a values of $[HRh(PP)_2(CH_3CN)]^{2+}$, correlate with poorer hydride donor abilities for $[H_2Rh(PP)_2]^+$ derivatives, and disfavor reductive elimination of H_2 from $[H_2Rh(PP)_2]^+$ complexes. Finally, larger cone angles decrease the pK_a of $[HRh(PP)_2(CH_3CN)]^{2+}$, decrease the hydride donor abilities of $[H_2Rh(PP)_2]^+$ derivatives, and favor reductive elimination of H_2 from $[H_2Rh(PP)_2]^+$. The coordination of acetonitrile that accompanies the protonation of $[Rh(PP)_2]^+$ and hydride transfer from *cis*-$[H_2Rh(PP)_2]^+$ to form *trans*-$[HRh(PP)_2(CH_3CN)]^{2+}$ results in increased steric interations between the coordinated acetonitrile ligands and the diphosphine ligands. As a result, these reactions are disfavored by an increase in both the NBA and the cone angle. Our results suggest that if solvent coordination is involved in hydride transfer and proton transfer reactions, the observed trends can be understood in terms of two different steric effects, NBAs, and cone angles, and in terms of electronic effects. It is important to emphasize that the two steric effects can be much larger than electronic effects, and that increasing cone angles and NBAs can have the same effect on thermodynamic properties, such as the acidity of $[HRh(PP)_2(CH_3CN)]^{2+}$ complexes and the hydricity of $[H_2Rh(PP)]^+$ complexes, or opposite effects, as in the reductive elimination of H_2 from $[H_2Rh(PP)]^+$ complexes. We believe that these concepts can be applied to a large range of proton and hydride transfer reactions in which solvent coordination is involved, and that they can help guide the development of a more comprehensive and quantitative understanding of the thermodynamic properties of these complexes.

Experimental Section

Syntheses. The $[Rh(PP)_2]^+$ complexes were prepared as yellow to orange powders following standard literature procedures.[18,58] In a representative preparation, a solution of the ligand dppp (2.15 g, 5.21 mmol) in 20 mL of MeCN was added to a 40 mL MeCN solution of $[Rh(COD)_2]OTf$ (1.22 g, 2.61 mmol), and the reaction mixture was allowed to stir for 2 h at room temperature. The volume of the solution was reduced to 10 mL under vacuum, and 100 mL of Et_2O added to produce a precipitate. The bright orange solid was collected by filtration, washed with 3 100 mL aliquots of petroleum ether, and dried in a vacuum for 12 h. The NMR data for this complex match the literature values reported for $[Rh(dppp)_2]OTf$ (2.73 g, 2.53 mmol, 97% yield).[58] The $^{31}P\{^1H\}$ NMR data and ^1H NMR hydride data also match the literature values for the remaining $[Rh(PP)_2]^+$ complexes used in this study, and these values are listed in Table 1.[18,22,58]

Equilibrium Measurements. All equilibrium measurements were made at 23 ± 2 °C by recording a series of NMR spectra on three to six different samples until the integration ratios became constant within experimental error. The standard state for H_2 is 1.0 atm, and the standard state for acetonitrile was taken as pure acetonitrile as discussed in the text.

Equilibria of $[Rh(dppe)_2][OTf]$ and $[Rh(dcpe)_2][OTf]$ with H_2 Gas at High Pressure. $[Rh(dppe)_2][OTf]$ (7 mg, 0.007 mmol) and 0.5 mL of CD_3CN were added to a sapphire NMR tube with a volume of 1.6 mL and fitted with a check valve which could be connected to a high pressure gas manifold. This tube was then charged with 1,754 psi (119 atm, ~4.8 mmol) of hydrogen with the pressure measured by a Wikall Transmitter UT-10 pressure gauge integrated into the manifold. Once charged, the NMR tube was inverted several times over a period of minutes to induce mixing. The reaction reached equilibrium within minutes as indicated by a constant ratio of NMR signals for products, $[Rh(dppe)_2][OTf]$ ($^{31}P\{^1H\}$ NMR: 58.5 ppm, int. set to 1.0) and $[H_2Rh(dppe)_2][OTf]$ ($^{31}P\{^1H\}$ NMR: 15.0 ppm, int. 0.104; −6.1 ppm, int. 0.104). The NMR was followed for at least 24 h to ensure the stability of the product ratio and vessel pressure. Integration of each of the resonances of $[H_2Rh(dppe)_2][OTf]$ and $[Rh(dppe)_2][OTf]$ as well as the pressure of the H_2 gas were used to calculate an equilibrium constant for Reaction 1 of 5.7×10^2 atm. A total of three experiments were conducted, each charged with hydrogen pressures between 1690 and 1760 psi (115−120 atm, 4.6−4.8 mmol). The integrals were measured, and an average $\Delta G°_{-H2}$ of −3.8 kcal/mol was calculated, with none of the values for individual experiments deviating more than 0.01 kcal/mol.

A similar series of three experiments were conducted for $[Rh(dcpe)_2][OTf]$, with hydrogen pressures between 1470 and 2060 psi (100−140 atm, 4.6−4.8 mmol). In the pressurized $[Rh(dcpe)_2][OTf]$ system, two major unknown side products were produced ($^{31}P\{^1H\}$ NMR: 92.6 ppm, d, $^1J_{RhP}$ 186 Hz; and 52.2 ppm, s) among other minor products in addition to the species attributed to $[H_2Rh(dcpe)_2][OTf]$. All species in the reaction mixture appeared to reach thermodynamically stable ratios within 24 h. The $[H_2Rh(dcpe)_2][OTf]$ species was identified by a hydride signal in the ^1H NMR spectrum at −12.5 ppm,

(58) Zhou, Z.; Facey, G.; James, B. R.; Alper, H. *Organometallics* **1996**, *15*, 2496–2503.

m, and by the $^{31}P\{^1H\}$ NMR: 74.6 ppm, m (P *cis* to hydride), 50.5 ppm, m, $^2J_{PH}$ ~140 Hz (P *trans* to hydride, assignment supported by $^{31}P-^1H$ HSQC). The relative concentrations of reactant and product were determined by integration of the signal assigned to $[Rh(dcpe)_2][OTf]$ and the signals associated with the phosphorus *cis* to hydride in $[H_2Rh(dcpe)_2][OTf]$. In this series of experiments, an average $\Delta G°_{-H2}$ of −4.2 kcal/mol was determined. None of the values for individual experiments deviated more than 0.05 kcal/mol. When $[Rh(dppb)_2][OTf]$ was exposed to high pressures, no reaction was observed.

Equilibrium of $[Rh(dppp)_2][OTf]$ with H_2 Gas. $[Rh(dppp)_2][OTf]$ (5 mg, 0.005 mmol) and 0.7 mL of CD_3CN were added to an NMR tube fitted with a septum. The tube was purged with a slow stream of H_2 for 10 min. The reaction reached equilibrium within minutes as indicated by a constant ratio of products, which persisted for more than 24 h. The species observed were $[Rh(dppp)_2][OTf]$ ($^{31}P\{^1H\}$ NMR: 8.4 ppm, d, $^1J_{RhP}$ 132 Hz) and $[H_2Rh(dppp)_2][OTf]$ ($^{31}P\{^1H\}$ NMR: 18.9 ppm, dt, $^1J_{RhP}$ 100 Hz, $^2J_{PP}$ 30 Hz; 7.0 ppm, dt, $^1J_{RhP}$ 83 Hz, $^2J_{PP}$ 30 Hz). The signals centered at 8.4 ppm ($[Rh(dppp)_2][OTf]$) and 7.0 ppm (half of total signal for $[H_2Rh(dppp)_2][OTf]$) were not resolved, so the combined integral of 1.2 was compared to the set integral of 1.0 for the signal at 18.8 ppm (the other half of $[H_2Rh(dppp)_2][OTf]$ total signal), giving a $[Rh(dppp)_2][OTf]/[H_2Rh(dppp)_2][OTf]$ ratio of 0.10. This value, combined with the hydrogen pressure of 1 atm, was used to calculate an equilibrium constant for Reaction 1 of 1.0×10^{-1} atm., and a $\Delta G°_{-H2}$ of 1.4 kcal/mol. A total of three experiments were conducted with no significant deviation in the integration ratios.

pK_a Determination of $[HRh(dmpe)_2(CH_3CN)][OTf]_2$ in Acetonitrile. In a typical experiment, $[Rh(dmpe)_2][OTf]$ (22.8 mg, 0.041 mmol), 1,8-bis(dimethylamino)naphthalene (proton sponge, ps, 51 mg, 0.24 mmol), and the triflate salt of protonated proton sponge (HpsOTf) (24 mg 0.066 mmol) were combined in an NMR tube with 0.6 mL of CD_3CN. The reaction was followed by ^{31}P NMR spectroscopy, and a constant ratio of $[HRh(dmpe)_2(CH_3CN)][OTf]_2$ (15.7 ppm, br; 3.4 ppm, br, int. set to 1) to $[Rh(dmpe)_2][OTf]$ (36.4 ppm, int. 0.85) was observed in less than 1 h. After correction for protonation of $[Rh(dmpe)_2][OTf]$, the ratio of H(ps)OTf/ps was determined to be 0.18 based on the initial mass added. Using these two ratios, an equilibrium constant of 1.5×10^{-1} was calculated for reaction 6. Combining this with the pK_a of protonated proton sponge in acetonitrile (18.2),[9] a pK_a of 18.9 can be calculated for $[HRh(dmpe)_2(CH_3CN)][OTf]_2$ using eq 9. This corresponds to a $\Delta G°_{H+}$ of 26.0 kcal/mol. Three independent experiments were performed in this manner, and $[HRh(dmpe)_2(CH_3CN)][OTf]_2$ was found to have an average pK_a of 18.9 and $\Delta G°_{H+}$ of 26.0 kcal/mol with none of the experiments deviating from the average by more than 0.16 kcal/mol.

pK_a Determination of $[HRh(depe)_2(CH_3CN)][OTf]_2$ in Acetonitrile. A similar set of three experiments was conducted for $[HRh(depe)_2(CH_3CN)][OTf]_2$ using the same proton sponge buffer system. For $[HRh(depe)_2(CH_3CN)][OTf]_2$ an average pK_a of 16.6 and $\Delta G°_{H+}$ of 22.8 kcal/mol were found; with none of the experiments deviating from the average by more than 0.05 kcal/mol.

pK_a Determination of $[HRh(depp)_2(CH_3CN)][OTf]_2$ in Acetonitrile. Using a anisidine buffer system (acetonitrile pK_a = 11.9)[44] prepared in an analogous way, another trio of experiments was conducted for $[HRh(depp)_2(CH_3CN)][OTf]_2$ to give an average pK_a value of 14.4 and $\Delta G°_{H+}$ of 19.8 kcal/mol, with none of the experiments deviating from the average by more than 0.04 kcal/mol. Use of 2,4-dichloroanilinium triflate as the acid produced the same chemical shifts as protonation with anisidinium triflate, supporting the formation of $[HRh(depp)_2(CH_3CN)][OTf]_2$ rather than $[HRh(depp)_2(base)][OTf]_2$.

pK_a Determination of $[HRh(dppp)_2(CH_3CN)][OTf]_2$ in Acetonitrile. The species $[Rh(dcpe)_2][OTf]$ and $[Rh(dppp)_2][OTf]$ required strong acids. In these cases acid/base buffers were prepared and injected as a solution into the NMR tube containing the complex and 0.6 mL of CD_3CN. A typical experiment involved adding trifluoromethanesulfonic acid (HOTf) (795 mg, 5.30 mmol) to dimethylformamide (DMF, pK_a = 6.1)[45] (966 mg, 13.2 mmol) to create a buffer with a ratio of H(DMF)OTf/DMF of 0.67. Then a portion of the buffer (167 mg, H(DMF)OTf, 0.51 mmol, DMF, 0.75 mmol) was injected into the NMR tube containing $[Rh(dppp)_2][OTf]$ (20 mg, 0.019 mmol). The reaction reached equilibrium within minutes as indicated by a constant ratio of products for more than 24 h. The products included $[Rh(dppp)_2][OTf]$ ($^{31}P\{^1H\}$ NMR: 8.4 ppm, d, $^1J_{RhP}$ 132 Hz, int. 0.66) to $[HRh(dppp)_2(CH_3CN)][OTf]_2$ ($^{31}P\{^1H\}$ NMR: 6.2 ppm, d, $^1J_{RhP}$ 91 Hz, int. set to 1.0). Considering the pK_a of H(DMF)OTf (6.1)[45] in acetonitrile and following the procedure set out above, a pK_a of 6.5 and $\Delta G°_{H+}$ of 8.8 kcal/mol were calculated. This experiment was conducted three times with a DMF buffer and three times with a dimethyl sulfoxide buffer (DMSO pK_a = 5.8)[45] to find that $[HRh(dppp)_2(CH_3CN)][OTf]_2$ had an average pK_a of 6.0 and $\Delta G°_{H+}$ of 8.7 kcal/mol with the maximum deviation for an individual experiment of 2.2 kcal/mol. Regardless of whether the acid was protonated DMSO or DMF, the same chemical shifts were observed for $[HRh(dppp)_2(CH_3CN)][OTf]_2$, suggesting that $[HRh(dppp)_2(base)][OTf]_2$ is not present in appreciable quantities.

pK_a Determination of $[HRh(dcpe)_2(CH_3CN)][OTf]_2$ in Acetonitrile. A similar series of experiments was conducted with $[Rh(dcpe)_2][OTf]$, three runs with a DMF buffer, and three runs with a dimethyl sulfoxide buffer. These experiments had the added challenge that $[Rh(dcpe)_2][OTf]$ decomposed into species identified as protonated dcpe and $[HRh(dcpe)(CH_3CN)_3][OTf]_2$ on exposure to strong acid. The addition of excess dcpe completely prevented the formation of $[HRh(dcpe)(CH_3CN)_3][OTf]_2$. Ignoring these side equilibria and focusing on the equilibrium between $[Rh(dcpe)_2][OTf]$, and $[HRh(dcpe)_2(CH_3CN)][OTf]_2$, and the buffer, it was found that $[HRh(dcpe)_2(CH_3CN)][OTf]_2$ had an average pK_a of 5.8 and $\Delta G°_{H+}$ of 7.9 kcal/mol with the maximum deviation for an individual experiment of 1.5 kcal/mol. Regardless of whether the acid was protonated DMSO or DMF, the same chemical shifts were observed for $[HRh(dcpe)_2(CH_3CN)][OTf]_2$, suggesting that $[HRh(dcpe)_2(Base)][OTf]_2$ is not present in appreciable quantities.

Equilibrium of $[HRh(depp)_2(CH_3CN)][OTf]_2$ with H_2 and Base. A solution of $[Rh(depp)_2][OTf]$ (22 mg, 0.033 mmol), anisidine (104 mg, 0.84 mmol), and anisidiniumOTf (31 mg, 0.11 mmol) (pK_a = 11.9)[44] in CD_3CN was prepared and sealed with a septum. This solution was bubbled with hydrogen twice a day for 2 days before reaching a stable equilibrium. The ratio of $[H_2Rh(depp)_2][OTf]$ and $[HRh(depp)_2(MeCN)][OTf]_2$ was determined from both the ^{31}P NMR and the ^1H NMR spectra. $^{31}P\{^1H\}$ NMR for $[HRh(depp)_2(MeCN)][OTf]_2$: 4.8 ppm, int 0.2, and for $[H_2Rh(depp)_2][OTf]$: 15.0 ppm, int. set to 1.0; −6.1 ppm int. 1.0. ^1H NMR for $[HRh(depp)_2(MeCN)][OTf]_2$: −17.6 ppm, int 0.5; and for $[H_2Rh(depp)_2][OTf]$: −10.8 ppm, int. set to 1.0. These data were used to calculate a value for K_{eq} of 1.3×10^{-2} for Reaction 10. The value of $\Delta G°_{H-}$ for $[H_2Rh(depp)_2][OTf]$ was determined to be 59.9 kcal/mol. This experiment was performed twice.

Another pair of experiments was performed with an aniline buffer (pK_a = 10.6)[46] prepared in a similar way as the DMSO and DMF buffers; however, the aniline was initially diluted in CD_3CN to prevent precipitation of the protonated amine. In these experiments a solution of $[Rh(depp)_2][OTf]$ in CD_3CN was prepared and sealed with a septum. One sample was first purged with hydrogen forming $[H_2Rh(depp)_2][OTf]$ as the dominant species. The buffer solution was added to this H_2-saturated solution, and an equilibrium mixture of $[H_2Rh(depp)_2][OTf]$ and $[HRh(depp)_2(MeCN)][OTf]_2$ was formed over a period of

2 days. The other tube was first injected with the buffer solution initially forming $[HRh(depp)_2(MeCN)][OTf]_2$ as the dominant species. This buffered solution was then purged with hydrogen for 10 min twice a day for 2 days, and progress toward equilibrium monitored. By averaging the values for all four experiments $[H_2Rh(depp)_2][OTf]$ was found to have a $\Delta G°_{H^-}$ of 61.3 kcal/mol with none of the experiments deviating from the average more than 1.1 kcal/mol.

Acknowledgment. This research was funded by BP through the Methane Conversion Cooperative (MC^2). D. L. DuBois would like to acknowledge the support of the Chemical Sciences program of the Office of Basic Energy Sciences, Division of Chemical Sciences, Biosciences and Geosciences of the Department of Energy and by the National Science Foundation. The Pacific Northwest National Laboratory is operated by Battelle for the U.S. Department of Energy.

Supporting Information Available: Derivation of Tolman cone angles for bidentate ligands used. This material is available free of charge via the Internet at http://pubs.acs.org.